

# We are IntechOpen, the world's leading publisher of Open Access books Built by scientists, for scientists

6,900

Open access books available

186,000

International authors and editors

200M

Downloads

Our authors are among the

154

Countries delivered to

TOP 1%

most cited scientists

12.2%

Contributors from top 500 universities



WEB OF SCIENCE™

Selection of our books indexed in the Book Citation Index  
in Web of Science™ Core Collection (BKCI)

Interested in publishing with us?  
Contact [book.department@intechopen.com](mailto:book.department@intechopen.com)

Numbers displayed above are based on latest data collected.  
For more information visit [www.intechopen.com](http://www.intechopen.com)



# Dielectrophoretic Deposition and Alignment of Carbon Nanotubes

Wei Xue and Pengfei Li

*Washington State University, Vancouver, WA  
U.S.A.*

## 1. Introduction

The carbon nanotube (CNT) is a unique form of carbon material. Since its discovery, CNT has been intensively studied due to its remarkable electrical, mechanical, thermal, and chemical properties (Iijima, 1991; Katz & Willner, 2004). Based on the structures and dimensions, CNTs can be divided into two groups: single-walled carbon nanotubes (SWNTs) and multi-walled carbon nanotubes (MWNTs). An SWNT is one tube of graphene capped at both ends and it consists of only surface carbon atoms; its diameter is in the range of 1-2 nm. An MWNT is composed of multiple coaxial tubes of SWNTs and its diameter is often in the range of 10-150 nm. CNTs have a high potential in a broad range of applications, especially in nanoelectronics and biomedical sensors. A wide variety of electronic devices based on individual CNTs or CNT thin films have been developed and used as sensors (Boul et al., 2009; Wang et al., 2009; Xue & Cui, 2008b), field-effect transistors (Xue & Cui, 2009; Xue et al., 2006), conductive interconnects (Robertson et al., 2008; Xue & Cui, 2008a), and energy storage systems (Hu et al., 2009; Kaempgen et al., 2009). A critical step to obtain these practical devices is to deposit well-organized and highly aligned CNTs in desired locations. Recently, researchers have developed a number of methods to align CNTs: using moving fluids to organize nanotubes (S. Li et al., 2007), introducing gas flows in reactors or channels (Liu et al., 2009), withdrawing microfluidic channels from solutions (Tsukruk et al., 2004), spin coating nanotube dispersions with controlled speeds (LeMieux et al., 2008; Roberts et al., 2009), and magnetic capturing of nanotubes (Shim et al., 2009). However, many of these techniques have limitations and restrictions because they require either intensive preparation processes or assisting materials with special properties. Therefore, their applications are relatively limited.

By comparison, dielectrophoresis, a simple but versatile method, has proven to be effective in aligning CNTs in small and large scales (Gultepe et al., 2008; Mureau et al., 2006). This method can be conducted at room temperature with low voltages. In addition, a number of parameters such as solution concentration, deposition time, alternating current (AC) amplitude, and frequency can be adjusted to optimize the quality of the aligned CNTs. More importantly, dielectrophoresis can be easily incorporated into device fabrication and has the potential to be used in wafer-level deposition for the mass production of CNT-based devices (Monica et al., 2008; Stokes & Khondaker, 2008; Xiao & Camino, 2009).

Recently, devices based on dielectrophoresis-aligned CNTs have been developed and used in various applications such as biocompatible substrates for cell growth (Yuen et al., 2008), bacteria capturing chips (Zhou et al., 2006), gas sensors (Lim et al., 2010), and memory devices (Di Bartolomeo et al., 2010). Numerical studies have also been performed to provide theoretical support of the process (Dimaki & Bøggild, 2004; Padmaraj et al., 2009). However, most of these research efforts are focused on the alignment of CNT thin films. Even though the controlled assembly of single CNT bundles has been studied by using various voltage magnitudes and types (Seo et al., 2005), a thorough investigation into the electrode geometry and the solution concentration is still necessary to achieve the deposition and alignment of individual CNTs and small nanotube bundles.

In this chapter, we examine the selective deposition of CNTs—including both SWNTs and MWNTs—with dielectrophoresis to obtain aligned nanotubes in the forms of thin films, small bundles, and individual nanotubes. These different results are obtained by changing the parameters in the dielectrophoresis process and the concentration of the CNT sample solutions. Pristine CNTs are treated with acids for surface functionalization and then diluted with deionized (DI) water to obtain different concentrations. The CNT thin films are deposited and aligned using a large-width electrode design; the alignment of nanotube bundles is achieved using a “teeth”-like electrode design; and the alignment of individual nanotubes is achieved using “teeth”-like electrodes with sharp tips. The “teeth”-like electrodes are used to generate a concentrated and highly directional electric field in between two opposite “teeth”. The electric field induces electric dipoles in CNTs and applies dielectrophoretic forces on them. Consequently, the dielectrophoretic forces move and rotate the CNTs to follow the electric field lines and eventually they land on the substrates to cover the electrodes. The electrodes are fabricated with optical lithography and wet etching; expensive equipment such as electron-beam writer—commonly used in the fabrication of individual nanotube devices—is avoided. The dielectrophoresis experiments are conducted at room temperature. Scanning electron microscopy (SEM) inspection shows that the CNTs are aligned in desired locations. The deposited SWNTs show better alignment than the MWNTs. Electrical characterization of the SWNT devices demonstrates that they have linear current-voltage ( $I$ - $V$ ) curves and their resistance is dependent on the SWNT solution concentration. For the MWNT devices, however, the  $I$ - $V$  curves are less linear. The material preparation, electrode design, fabrication process, dielectrophoresis process, quality of the aligned nanotubes and thin films, microscope observation, and electrical characterization of the thin-film devices are described and discussed in this chapter.

## 2. Materials and experiments

The CNTs—both SWNTs and MWNTs—used in our experiments are purchased from SES Research (Houston, TX). The pristine CNTs are in the form of powder; the specifications for the SWNTs are: outer diameter < 2 nm, length 5-15  $\mu\text{m}$ , purity > 90%; the specifications for the MWNTs are: outer diameter 60-100 nm, length 5-15  $\mu\text{m}$ , purity > 95%. Because dielectrophoresis is a solution-based method, it requires that the deposited materials used in the process are free to move and rotate in a medium. However, it is well known that the pristine CNTs suffer from poor solubility in most solvents. Therefore, to increase the solubility and processability of CNTs, defects such as terminal groups can be intentionally introduced to their sidewalls and open ends with various chemical oxidation methods (Banerjee et al., 2005).

In our study, the pristine CNTs are chemically functionalized with a mixture of sulfuric and nitric acids (3:1  $\text{H}_2\text{SO}_4:\text{HNO}_3$ ) at  $110^\circ\text{C}$  for 45 min. The mixture of acids cuts the CNTs into short tubes with openings at both ends, as shown in Fig. 1. The acid treatment introduces the covalent attachment of carboxylic (-COOH) groups on the surfaces and open ends of CNTs. As a result, the CNTs can be uniformly dispersed in DI water and remain stable for a long period of time (10-12 months). In addition, the nitric acid in the mixture can purify the CNTs by removing amorphous carbon, carbon particles, and other impurities.

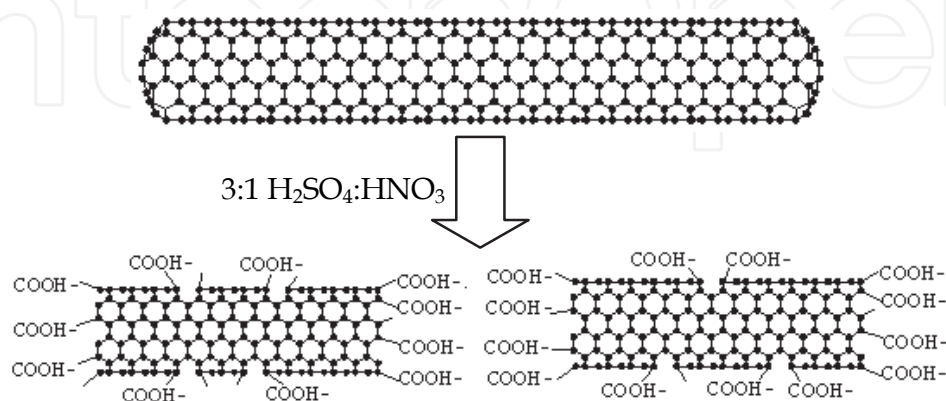


Fig. 1. Scheme of the chemical functionalization of a SWNT. The SWNT is cut into short tubes with carboxylic groups covalently attached to the sidewalls and open ends.

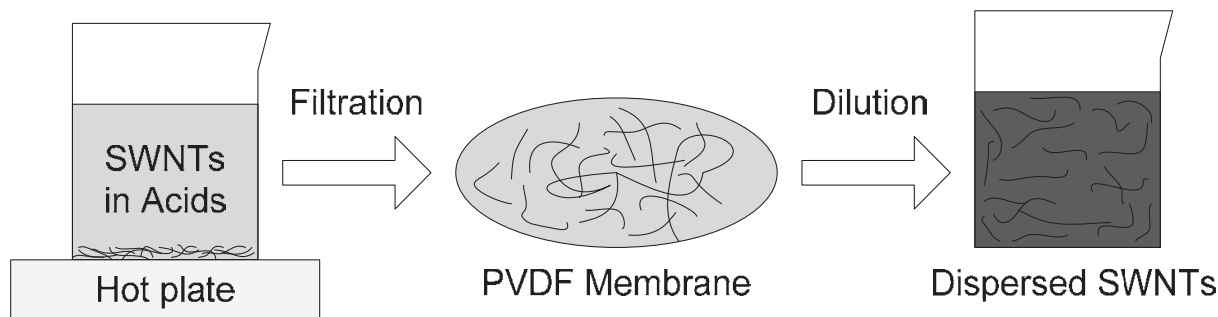


Fig. 2. Surface functionalization process of the CNTs with acid treatment, filtration, and dilution.

After the acid treatment, the functionalized CNTs are diluted with DI water and filtered with a polyvinylidene fluoride (PVDF) filtration membrane (with an average pore diameter of  $0.22\ \mu\text{m}$ ) repeatedly for 5-6 times until the pH value of the dispersion reaches five. Next, the purified and functionalized CNTs are collected from the PVDF membrane and dispersed in DI water. The CNT dispersion is treated with an ultrasonic process for 30 min to obtain a more uniform solution. Last, the dispersed CNTs are diluted with DI water to obtain different concentrations: 0.2, 0.1, 0.05, 0.025, and 0.0125 mg/ml for SWNT solutions and 0.1, 0.05, 0.025, 0.0125, and 0.00625 mg/ml for MWNT solutions. These concentrations are selected because the samples can show clear differences after the nanotube deposition. Figure 2 shows the process flow to obtain the diluted CNT solutions.

To investigate the deposition and alignment of CNTs in various configurations, two types of electrodes are designed and fabricated (P. Li & Xue, 2010a). The first electrode design is used for the deposition of thin films. In this design, the electrodes have a large width of 400

$\mu\text{m}$  and a gap of  $5 \mu\text{m}$ . The schematic structure of the design and an SEM image of the fabricated electrodes are shown in Fig. 3. When an AC signal is applied on the device, an alternating electric field with parallel lines is generated in between the electrodes. The CNTs in the dispersion can be attracted to this area by the dielectrophoretic force. They are re-oriented to follow the electric field lines and evenly distributed across the width of the electrodes after deposition.

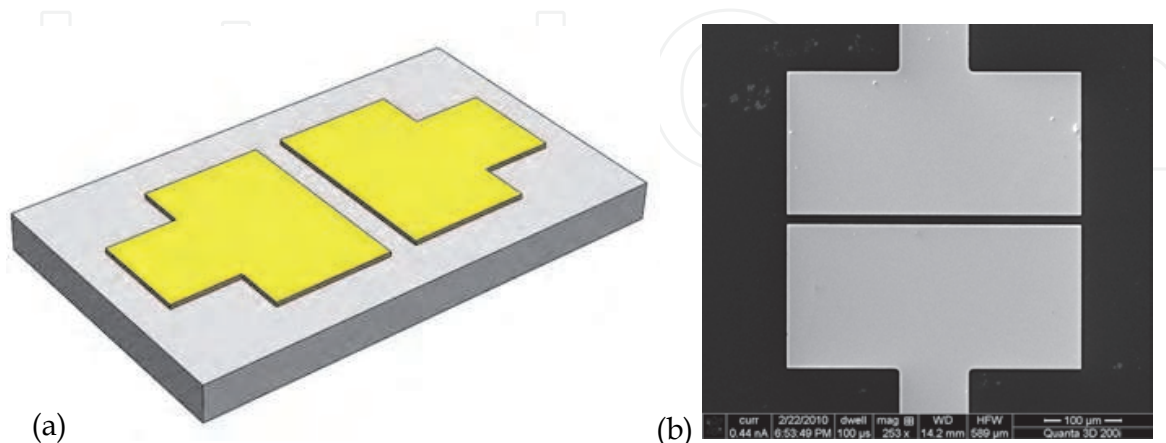


Fig. 3. (a) Schematic structure of the wide electrode design. The width and the gap of the electrodes are  $400$  and  $5 \mu\text{m}$ , respectively. (b) An SEM image of the fabricated electrodes. Reprinted with permission from P. Li & Xue, 2010a. © 2010 Springer.

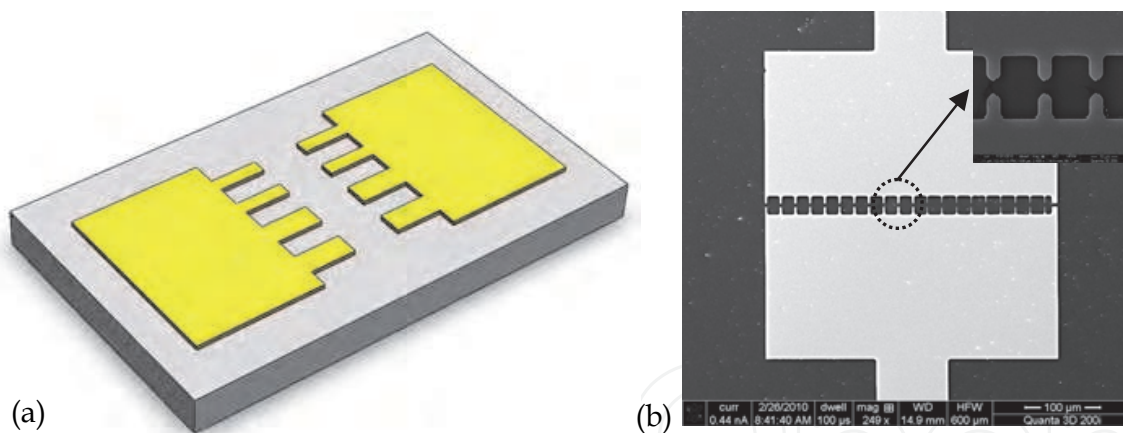


Fig. 4. (a) Schematic structure of the “teeth”-like electrode design. The electrodes have two different widths of  $5$  and  $3 \mu\text{m}$ . The gap between the electrodes is  $3 \mu\text{m}$ . (b) An SEM image of the fabricated electrodes. The enlarged area shows the electrode pairs with sharp tips. Reprinted with permission from P. Li & Xue, 2010a. © 2010 Springer.

The second electrode design is used for the deposition and alignment of sparsely distributed nanotubes, nanotube bundles, and individual nanotubes. The electrodes are designed as “teeth”-like structures with a  $3\text{-}\mu\text{m}$  gap in between, as shown in Fig. 4. The “teeth”-like electrode design enables a highly concentrated electric field in desired regions. In order to control the electric field strength and distribution profile, the electrodes are designed to have two different widths of  $5$  and  $3 \mu\text{m}$ . The  $5\text{-}\mu\text{m}$ -wide electrodes are used for the alignment of sparsely distributed nanotubes; the  $3\text{-}\mu\text{m}$ -wide electrodes are used for the alignment of nanotube bundles and individual nanotubes.

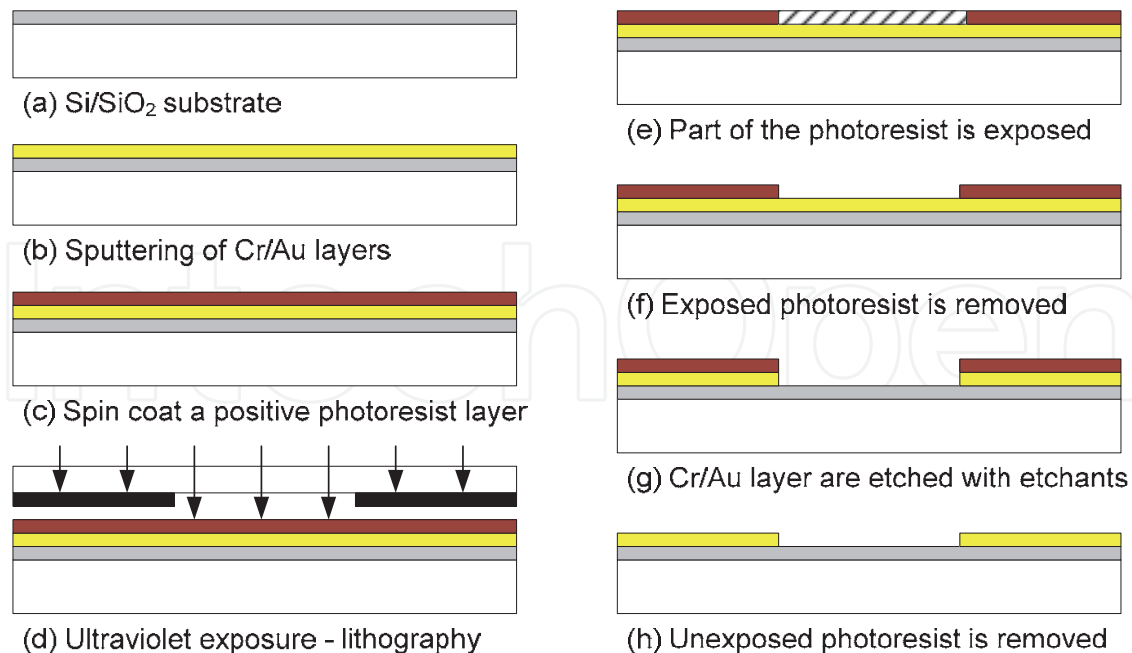


Fig. 5. Fabrication process of the electrodes using optical lithography and wet etching.

The electrodes are fabricated on 4-inch silicon wafers. The wafers are covered with a 200-nm-thick thermal-grown  $\text{SiO}_2$  insulating layer. Metal layers of Cr (100 nm, adhesion material) and Au (200 nm, electrode material) are coated on the wafer surface with sputtering. One of the biggest advantages of dielectrophoresis in nanotube alignment is its high potential in wafer-level deposition, which is compatible with the parallel micro/nano-fabrication processes used in the semiconductor industry. Therefore, series (and often expensive) nanofabrication processes using equipment such as electron-beam lithography and scanning-probe lithography should be avoided. In our investigation, the entire fabrication process is compatible with the traditional microfabrication technology, as shown in Fig. 5. We use optical lithography with a hard contact aligner (OAI 200 Mask Aligner), a positive photoresist (Shipley S1813), and controlled wet etching to obtain electrodes, which can generate electric field with desired strength and distribution. The parameters for the etching steps are 120 sec for Cr etching using a standard chromium mask etchant and 20 sec for Au etching using a gold etchant (Type TFA from Transene Inc.). After the controlled etching steps, the actual widths of the electrodes are reduced to 2-3 (designed width: 5  $\mu\text{m}$ ) and 0.5-1  $\mu\text{m}$  (designed width: 3  $\mu\text{m}$ ). Figure 6 shows an optical image of a fabricated device. The dimensions of the device are 75 mm  $\times$  75 mm, smaller than a dime. The center of the device contains the electrodes used for the dielectrophoresis process. The electrodes are elongated to the edge of the device as probing pads for the application of the AC signal.

### 3. Dielectrophoresis

When dielectric particles are exposed to a non-uniform electric field, charges including electrons (-) and protons (+) are moved away from their initial balanced positions and redistributed in these particles. The charge redistribution creates electric dipole moments which force these particles to rotate along the electric field lines. The induced effective dipole moment for an ellipsoidal particle can be expressed as (Peng et al., 2006):

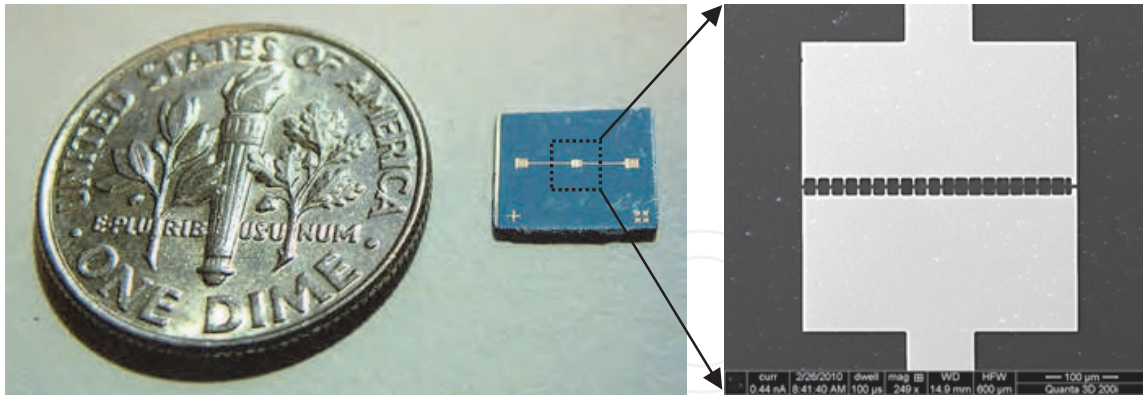


Fig. 6. Optical image of a fabricated device next to a dime.

$$p_{eff} = \frac{V(\epsilon_p - \epsilon_m)E}{[1 + (\epsilon_p - \epsilon_m) / \epsilon_m]A_L} \quad (1)$$

where  $V$  is the volume of the particle,  $\epsilon_p$  and  $\epsilon_m$  are the permittivities of the particle and the medium,  $E$  is the external electric field strength,  $A_L \approx 4r^2/l^2[\ln(l/r)-1]$  is the depolarization factor, and  $r, l$  are the radius and length of the ellipsoidal particle, respectively.

Similarly, an external non-uniform electric field can induce dipole moments in rod-like objects including nanowires and carbon nanotubes. The dipole moment parallel to the tube axis is much stronger than that in the perpendicular direction. Therefore, the polarized nanotube, if free to move in a medium, is subject to a net force and can be aligned to follow the electric field direction, as shown in Fig. 7.

The net force exerted on the nanotube is expressed as (Dimaki & Bøggild, 2004; Raychaudhuri et al., 2009):

$$F = \frac{\pi r^2 l}{6} \epsilon_m \text{Re}[f_{cm}] |\nabla E_{rms}^2| \quad (2)$$

where the term  $r^2 l / 6$  is a geometry factor that contains the volume information of the nanotube,  $\text{Re}[f_{cm}]$  is the real number part of the Clausius-Mossotti factor  $f_{cm}$ , and  $|\nabla E_{rms}^2|$  is the root mean square of the gradient of the external electric field. When the long axis of the nanotube is aligned along the electric field line, the Clausius-Mossotti factor  $f_{cm}$  can be derived from (Ahmed et al., 2009; Dimaki & Bøggild, 2004):

$$f_{cm}(\text{long axis}) = \frac{\epsilon_n^* - \epsilon_m^*}{(\epsilon_n^* - \epsilon_m^*)A_L + \epsilon_m^*} \quad (3)$$

where  $A_L$  is the depolarization factor along the long axis, the subscripts  $n$  and  $m$  represent the nanotube and the medium, respectively, and  $\epsilon^*$  is the complex permittivity that contains the information of the physical permittivity  $\epsilon$ , the conductivity  $\sigma$ , and the angular velocity of the external electric field  $\omega$ . The term  $\epsilon^*$  is defined as:

$$\epsilon^* = \epsilon - j \frac{\sigma}{\omega} \quad (4)$$

These equations indicate that the dielectrophoresis of CNTs is affected by many factors including the dimensions of the nanotubes, the properties of the medium, and the strength of the electric field. In our investigation, the following parameters are adjusted to control the deposition and alignment of the nanotubes: bias voltage, frequency, deposition time, width of the electrodes, and nanotube solution concentration.

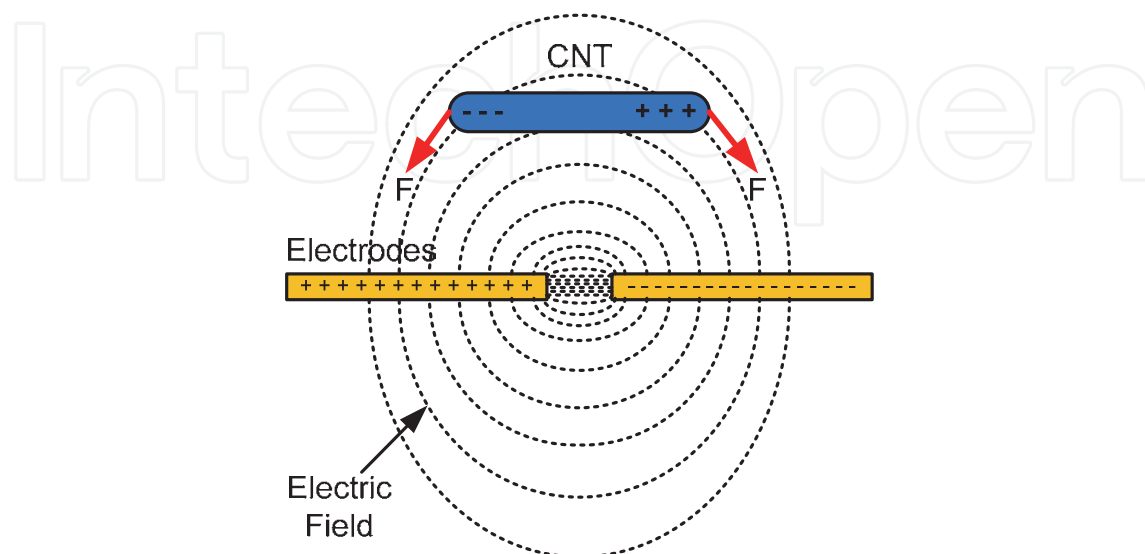


Fig. 7. Principle of dielectrophoresis deposition and alignment of a carbon nanotube.

Early research demonstrates that the polarization along the longitudinal direction is much higher than that along the transverse direction for metallic CNTs, but comparable for semiconducting CNTs (Padmaraj et al., 2009). This is because the metallic CNTs have a larger  $Re[f_{cm}]$  and the dielectrophoretic force exerted on them is much stronger than that experienced by the semiconducting CNTs. Therefore, we expect that the metallic CNTs will dominate the movement of SWNT bundles in the dielectrophoresis process in our experiments.

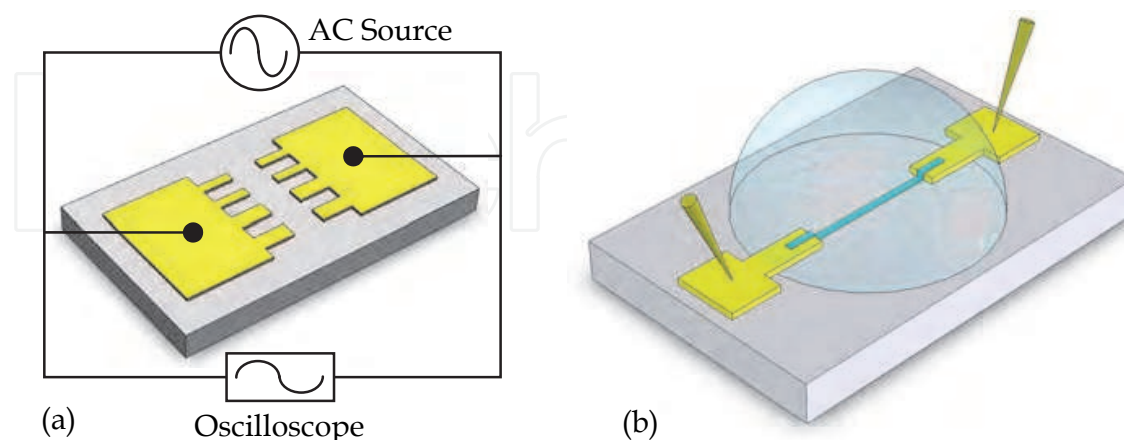


Fig. 8. (a) Experimental system for the dielectrophoresis of CNTs. (b) Schematic diagram of the CNT alignment. Reprinted with permission from P. Li & Xue, 2010a. © 2010 Springer.

Figure 8a shows the configuration of the experimental system for the dielectrophoresis of the CNTs. A function generation (Agilent Technologies 81150A) is used as the AC signal

source and it is connected to the electrodes through two metal probes. The potential drop across the electrode gap is monitored with an oscilloscope (Agilent Technologies MSO 7054A), which provides the voltage value in real time. After the instruments are set up, a droplet of the CNT solution is carefully placed in the area between the electrodes with a syringe. Next, the AC signal source is switched on. An electric field is generated in between the electrode “teeth”. The electric field exerts dielectrophoretic forces on the CNTs and forces them to rotate along the field lines. The CNTs can be deposited on the substrate with this orientation, as shown in Fig. 8b. After 30 sec of dielectrophoresis, the AC signal is switched off and the CNT solution is removed with another syringe. The experiments are conducted at room temperature with an applied AC signal with a peak-to-peak voltage of  $V_{pp} = 10$  V and frequency of  $f = 5$  MHz.

## 4. Results and discussion

In the dielectrophoresis process, the dielectrophoretic forces drag the CNTs to the gap of the electrodes where the electric field has the highest magnitude. In reality, however, the dielectrophoresis process and the deposition results of the CNTs are affected by a number of factors including the dimensions of the nanotubes, the properties of the medium, and the strength of the electric field. In this research, the alignment results of the two forms of CNTs—SWNTs and MWNTs—are investigated and compared. In addition, the electrical properties of these resulting CNTs are studied.

### 4.1 SWNTs

As described earlier, the fabricated devices can be divided into three groups: 400- $\mu\text{m}$ -wide electrodes, 5- $\mu\text{m}$ -wide electrodes, and 3- $\mu\text{m}$ -wide electrodes. For each group, the electrodes are exposed to the SWNT solutions with different concentrations, ranging from 0.2 to 0.00125 mg/ml. An SEM (FEI Quanta 3D 200i) is used to inspect the deposited SWNTs after the dielectrophoresis process. A semiconductor device analyzer (Agilent Technologies B1500A) is used to characterize the electrical properties of the aligned SWNTs.

#### 4.1.1 Deposition and alignment of the SWNTs

Figure 9 shows the SEM images of the deposited SWNTs on the substrates with the 400- $\mu\text{m}$ -wide electrodes. This electrode design enables an evenly distributed electric field with parallel field lines in the gap. The SWNTs are stretched and aligned in between the electrodes to follow the parallel field lines. The density of the SWNT thin film is dependent on the concentration of the SWNT solution used in the dielectrophoresis process. A higher solution concentration induces a denser SWNT film. The alignment experiments are highly repeatable when used to fabricate SWNT thin films. However, it is difficult to obtain small nanotube bundles or individual nanotubes using this group of devices.

In order to explore the possibility of producing aligned nanotube bundles and individual nanotubes, narrower electrodes are used. Figure 10 shows the SEM images of the aligned SWNTs on the devices with the 5- $\mu\text{m}$ -wide electrodes. Figure 10a demonstrates a dense film of SWNTs covering the electrode gap, where most SWNTs are aligned to follow the direction of the electric field lines. As the solution concentration decreases, fewer SWNTs are attracted by the dielectrophoretic force and deposited on the substrate. In addition, the SEM inspection shows that there are no SWNTs observed outside the electrode gap area.

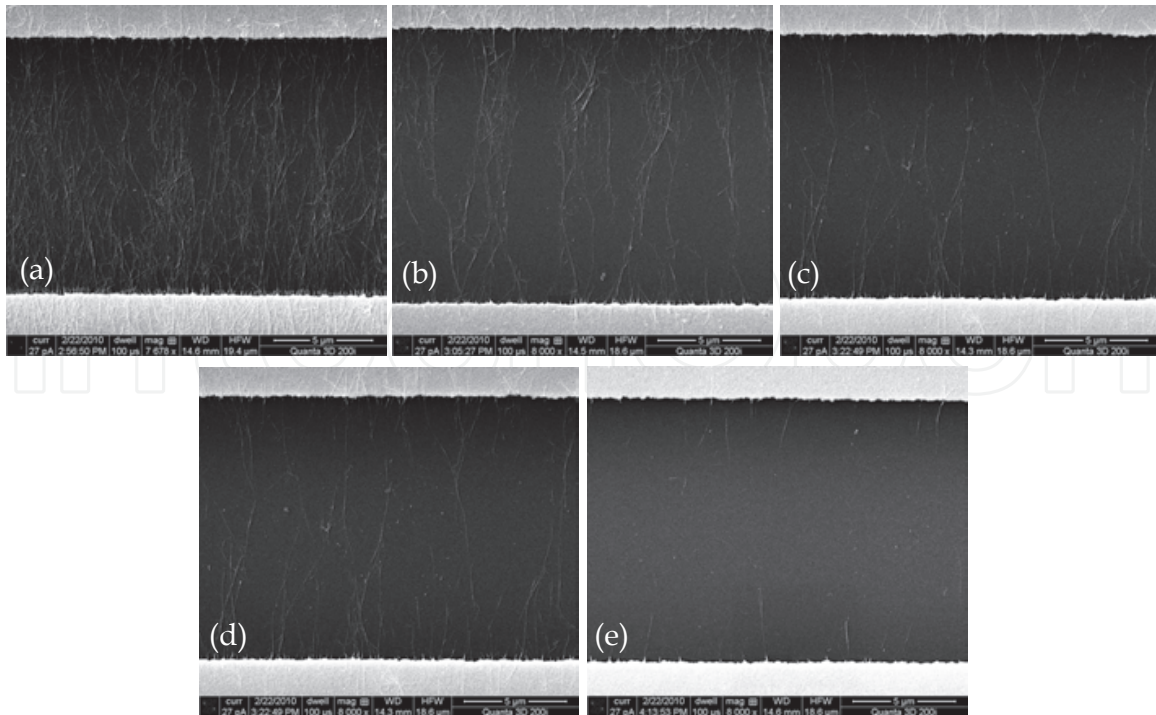


Fig. 9. SEM images of aligned SWNTs with the 400- $\mu$ m-wide electrodes and solutions with different concentrations: (a) 0.2 mg/ml, (b) 0.1 mg/ml, (c) 0.05 mg/ml, (d) 0.025 mg/ml, and (e) 0.0125 mg/ml. Reprinted with permission from P. Li & Xue, 2010a. © 2010 Springer.

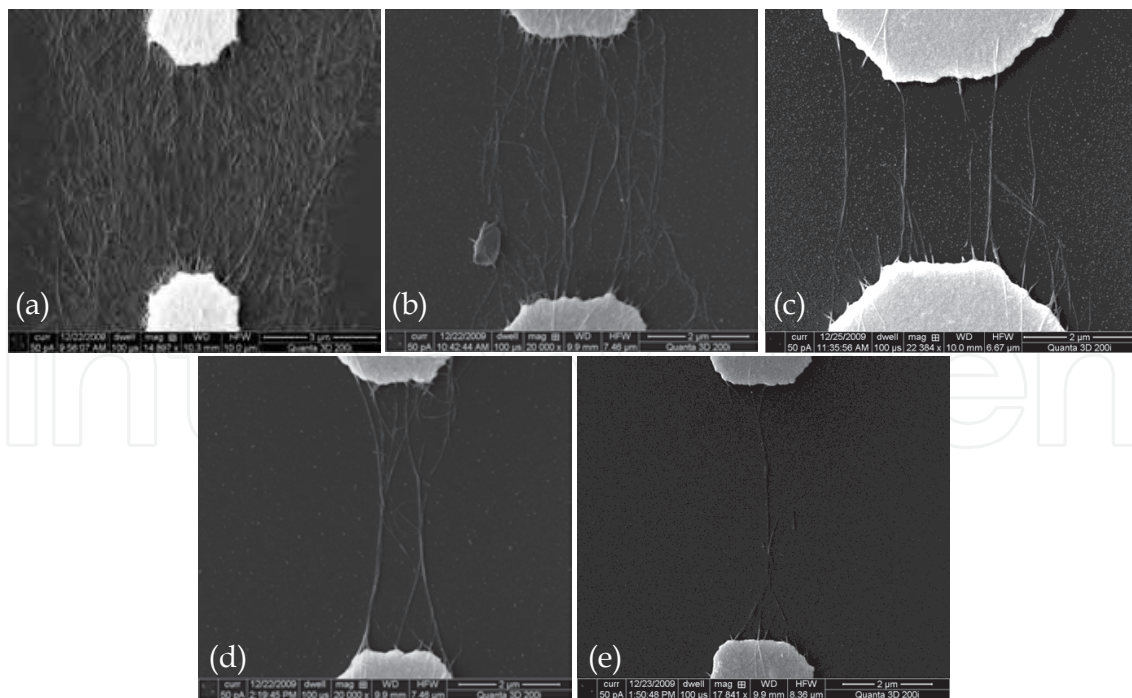


Fig. 10. SEM images of aligned SWNTs with the 5- $\mu$ m-wide electrodes and solutions with different concentrations: (a) 0.2 mg/ml, (b) 0.1 mg/ml, (c) 0.05 mg/ml, (d) 0.025 mg/ml, and (e) 0.0125 mg/ml. Reprinted with permission from P. Li & Xue, 2010a. © 2010 Springer.

This proves that the dielectrophoresis process is a selective deposition technique which only moves SWNTs to areas with strong electric fields. Figure 10b-d show sparsely distributed nanotube bundles and Fig. 10e shows a small bundle of SWNTs. Compared with the devices with wider electrodes (Fig. 9), the devices with 5- $\mu\text{m}$ -wide electrodes can generate a more concentrated electric field in the gap and force the SWNTs to land on the substrate to cover a smaller area. The bundling phenomenon of the SWNTs in the solution is caused by their high aspect ratios and high flexibility. Based on Fig. 10b-e, as the solution concentration decreases, the bundles become thinner due to the lower availability of SWNTs in the solution.

For the narrowest electrodes with the width of 3  $\mu\text{m}$ , the quality of the deposition and alignment of SWNTs is similar to that for the electrodes with 5- $\mu\text{m}$  width, as shown in Fig. 11. However, there are three major differences comparing the results from the two designs. First, the amount of the aligned SWNTs on the 3- $\mu\text{m}$ -wide electrodes is smaller. This is because the area with a strong and concentrated electric field, generated by the narrower electrodes, is smaller. Second, the bundles deposited on the 3- $\mu\text{m}$ -wide electrodes are thinner and contain smaller numbers of nanotubes. Third, and most importantly, individual nanotubes can be observed in the dielectrophoresis experiments using low-concentration solutions and 3- $\mu\text{m}$ -wide electrodes (Fig. 11e). In this case, the narrow electrode design ensures that the electric field in between the electrodes is extremely concentrated and highly directional. The low solution concentration ensures that in the adjacent area there is only one nanotube available in the solution to be attracted by the electric field. Consequently, this individual nanotube is deposited on the substrate and aligned in between the electrodes.

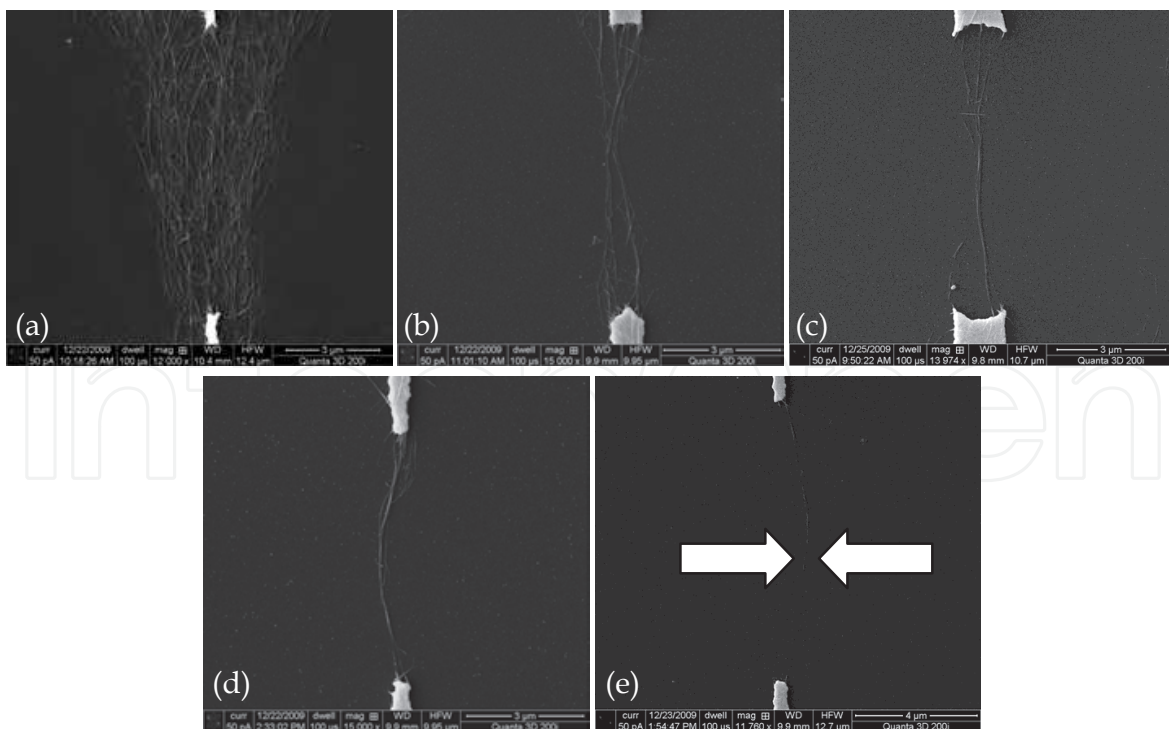


Fig. 11. SEM images of aligned SWNTs with the 3- $\mu\text{m}$ -wide electrodes and solutions with different concentrations: (a) 0.2 mg/ml, (b) 0.1 mg/ml, (c) 0.05 mg/ml, (d) 0.025 mg/ml, and (e) 0.0125 mg/ml. Reprinted with permission from P. Li & Xue, 2010a. © 2010 Springer.

#### 4.1.2 Electrical characteristics of the aligned SWNTs

After the dielectrophoresis process, the gap of the electrodes are covered with the deposited and aligned SWNTs, which allows the transmission of electric charges across the electrodes. As a result, these devices can be measured as regular resistors with the electrodes as the testing pads and the aligned SWNTs as the conductive path (P. Li & Xue, 2010b). To gain a better understanding of the effects of the solution concentration on the deposition and alignment of SWNTs, the electrical properties of the devices after the dielectrophoresis process are characterized with the semiconductor device analyzer. Based on the design of the electrodes, the devices are divided into two groups: the first group contains devices with the wide electrodes (width: 400  $\mu\text{m}$ ) and the second group includes devices with the “teeth”-like electrodes (width: 5  $\mu\text{m}$  and 3  $\mu\text{m}$ ). Each group consists of five different SWNT devices corresponding to the solutions used in the dielectrophoresis process.

The electrical properties of the wide-electrode devices are illustrated in Fig. 12a. The width and the gap of the electrodes are 400 and 5  $\mu\text{m}$ , respectively. These devices are measured as regular resistors with the current-voltage plots as the output characteristics. In the measured range of -3 to 3 V, all plots are highly linear. The resistances of these devices are calculated accordingly and plotted in Fig. 12b. At a low SWNT solution concentration of 0.0125 mg/ml, which corresponds to the device shown in Fig. 9e, only a few SWNTs are captured. The resistance is measured as approximately 35.015 k $\Omega$ . As the concentration increases, the resistance quickly decreases to a lower value and remains relatively constant in a low-resistance region. The calculated resistances are 23.641 k $\Omega$  (SWNT solution: 0.025 mg/ml), 0.832 k $\Omega$  (SWNT solution: 0.05 mg/ml), 0.099 k $\Omega$  (SWNT solution: 0.1 mg/ml), and 0.035 k $\Omega$  (SWNT solution: 0.2 mg/ml).

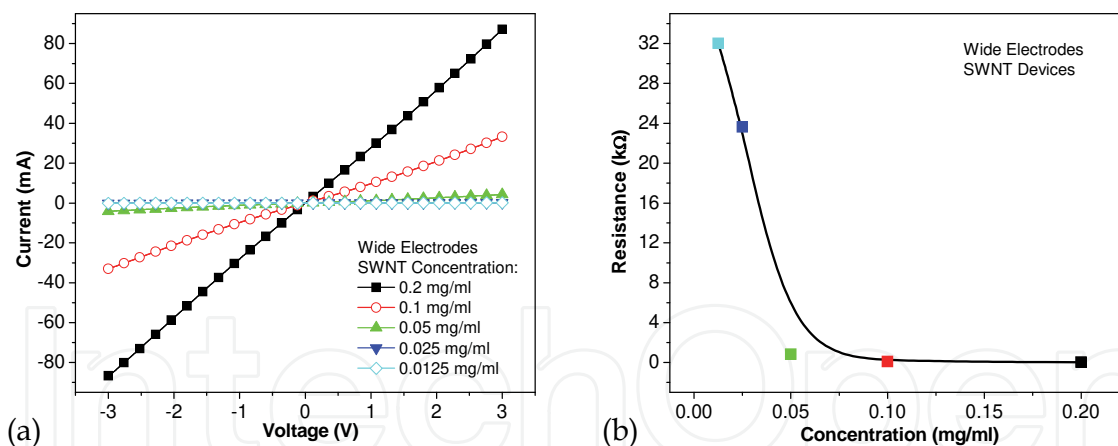


Fig. 12. (a) Current-voltage plots of five devices with the 400- $\mu\text{m}$ -wide electrodes using SWNT solutions with different concentrations. (b) Resistance as a function of the concentration for the aligned SWNTs. The resistances are calculated from (a). Reprinted with permission from P. Li & Xue, 2010b. © 2010 American Society of Mechanical Engineers.

The electrical characteristics of the devices with the “teeth”-like electrodes are obtained using the same method. The devices are based on the second electrode design which contains electrodes with variable widths (Fig. 4). Each device consists of eleven 5- $\mu\text{m}$ -wide electrode pairs and nine 3- $\mu\text{m}$ -wide electrode pairs. Figure 13a shows the  $I$ - $V$  plots of five devices using SWNT solutions with five different concentrations. In the measured range of -3 and 3 V, all five  $I$ - $V$  plots are highly linear. Figure 13b shows the calculated resistance as a

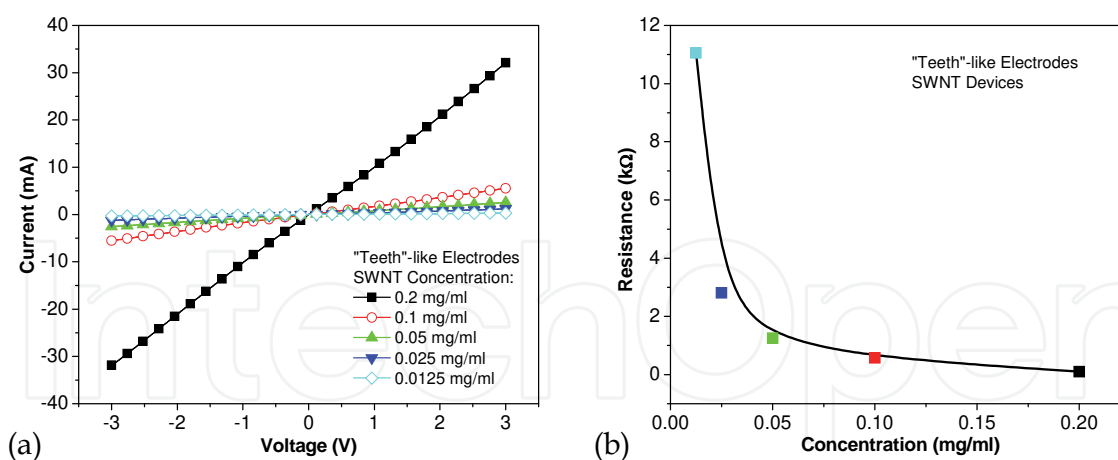


Fig. 13. (a) Current-voltage plots of five devices with the “teeth”-like electrodes using SWNT solutions with different concentrations. (b) Resistance as a function of the concentration for the aligned SWNTs. The resistances are calculated from (a). Reprinted with permission from P. Li & Xue, 2010a. © 2010 Springer.

function of the solution concentration. The resistance of the device starts as 11.055 kΩ at the lowest concentration (SWNT solution: 0.0125 mg/ml) and quickly decreases to 2.806 kΩ (SWNT solution: 0.025 mg/ml). It continues to decrease to lower values of 1.256 kΩ (SWNT solution: 0.05 mg/ml), 0.571 kΩ (SWNT solution: 0.1 mg/ml), and 0.097 kΩ (SWNT solution: 0.2 mg/ml). Although this group of devices shows a similar resistance-concentration relationship to the first group of devices with wide electrodes, the resistance range is different. For example, the largest obtained resistances are 11.055 and 32.015 kΩ for the “teeth”-like and wide electrodes, respectively. This difference is caused by the different amount of aligned SWNTs on the substrates. The devices with wide electrodes are able to capture more SWNTs, providing more conductive paths for the charges to move across the electrodes. As a result, these devices show lower resistance.

The characterization of these devices verifies the results from the SEM inspection and proves that the higher-concentration solutions lead to denser films with more deposited SWNTs. The high linearity of the  $I$ - $V$  plots suggests that the aligned SWNTs are mostly metallic nanotubes instead of semiconducting nanotubes. These experimental results fit well with the prediction described in Section 3: Dielectrophoresis.

## 4.2 MWNTs

The deposition, alignment, and electrical characteristics of the MWNTs are investigated using the same procedures as those for the SWNTs. The experiment and measurement results of the aligned MWNTs are described; the main differences between the deposited MWNTs and SWNTs are discussed.

### 4.2.1 Deposition and alignment of the MWNTs

The alignment results of the MWNTs are similar to those for the SWNTs – the solutions with higher MWNT concentrations generate denser films, as shown in Fig. 14. However, most MWNTs are tangled together and are not fully stretched in between the electrodes. This can be explained by the special dimensions and structures of the MWNTs. First, the typical diameter of the MWNTs used in our experiments is 60-100 nm, which is much larger than

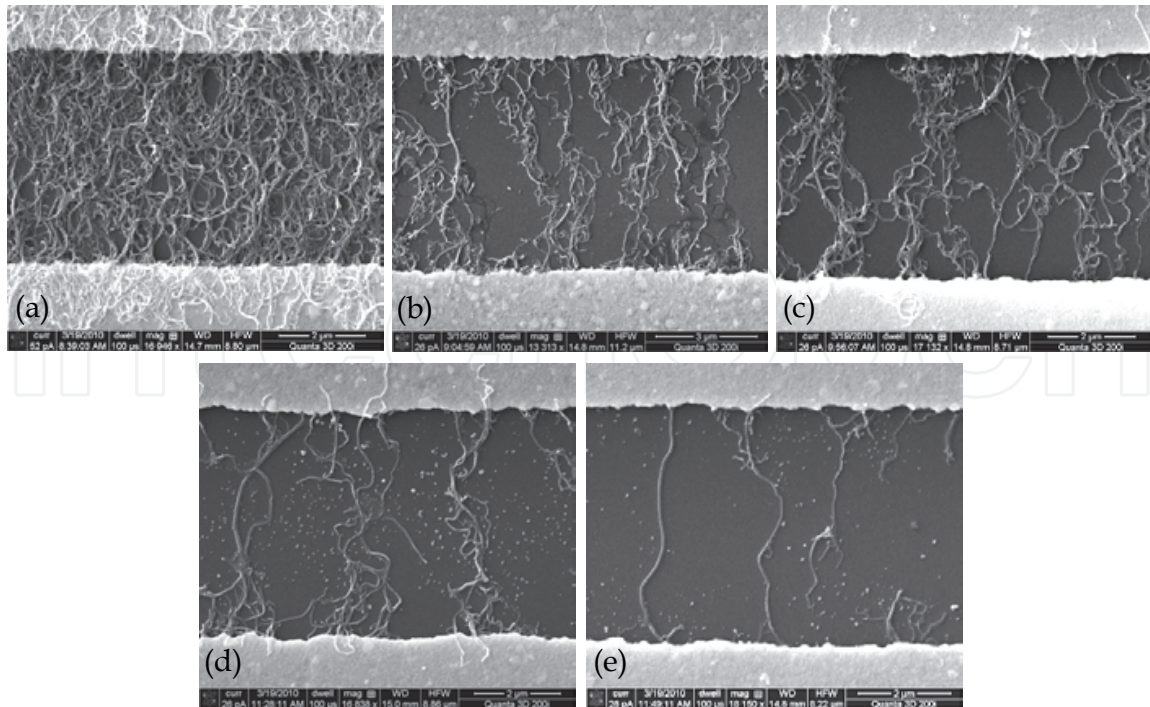


Fig. 14. SEM images of aligned MWNTs with the 400- $\mu$ m-wide electrodes and solutions with different concentrations: (a) 0.1 mg/ml, (b) 0.05 mg/ml, (c) 0.025 mg/ml, (d) 0.0125 mg/ml, and (e) 0.00625 mg/ml.

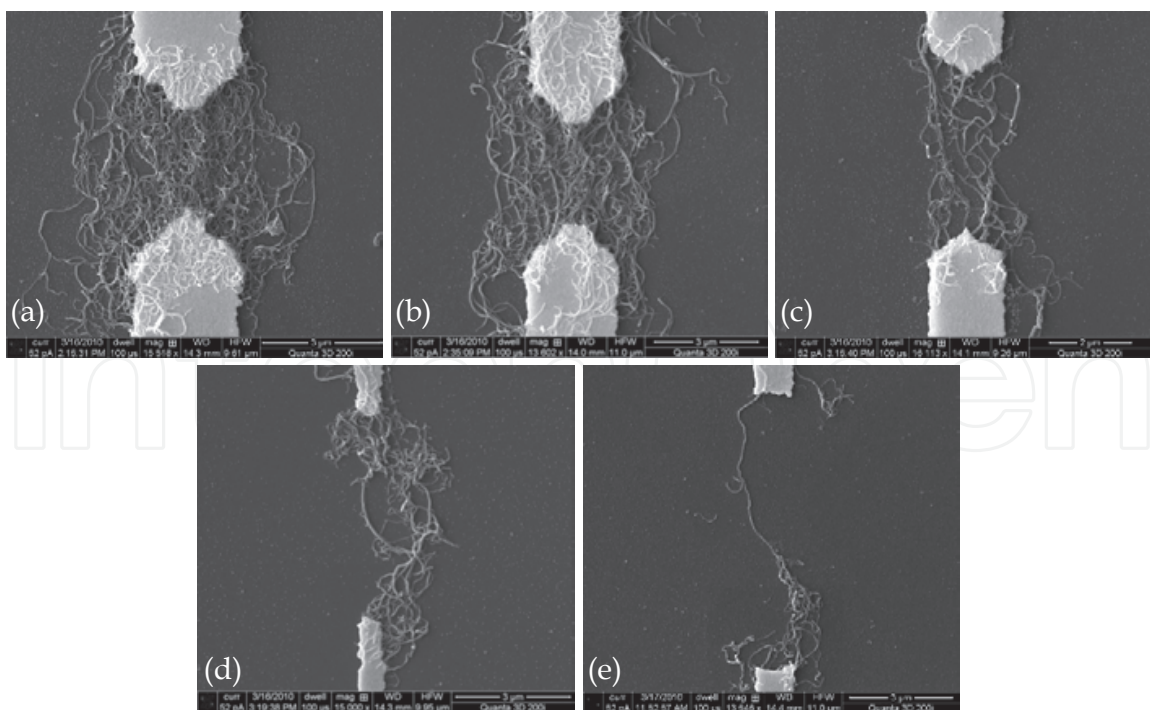


Fig. 15. SEM images of aligned MWNTs with the "teeth"-like electrodes and solutions with different concentrations: (a) 0.1 mg/ml, (b) 0.05 mg/ml, (c) 0.025 mg/ml, (d) 0.0125 mg/ml, and (e) 0.00625 mg/ml.

that of the SWNTs (2 nm). Second, the multi-walled structure of the MWNTs makes their mechanical properties different from the SWNTs – the MWNTs are heavier and stiffer. As a result, when the MWNTs are exposed to an external electric field, the generated dielectrophoretic forces are not strong enough to fully stretch the MWNTs. Furthermore, the thin films generated from the solutions with higher MWNT concentrations have a higher degree of randomness. As the concentration decreases to a lower level, the MWNTs are suspended in the solution more homogeneously and their interaction with each other becomes weaker. Therefore, the resulting films and bundles are more organized with better quality of alignment.

The “teeth”-like electrodes are also used for the dielectrophoretic assembly of the MWNTs, as shown in Fig. 15. Unlike the wide electrodes, the “teeth”-like electrodes only generate high-gradient electric field between two opposite “teeth”. Consequently, the MWNTs are only deposited in these locations. Similar to the experimental results of the SWNT samples, the MWNTs only deposit in between the electrodes. In addition, we are able to achieve not only the deposition of narrow-width thin films, but also the assembly of a controlled amount of MWNTs or even individual MWNTs, as demonstrated in Fig. 15e.

#### 4.2.2 Electrical characteristics of the aligned MWNTs

The electrical characterization of the MWNTs deposited on the electrodes is performed after the dielectrophoresis process. The devices are divided into two groups: the first group contains devices with the wide electrodes (width: 400  $\mu\text{m}$ ) and the second group includes devices with the “teeth”-like electrodes. Each group consists of five different MWNT devices corresponding to the solutions used in the dielectrophoresis process.

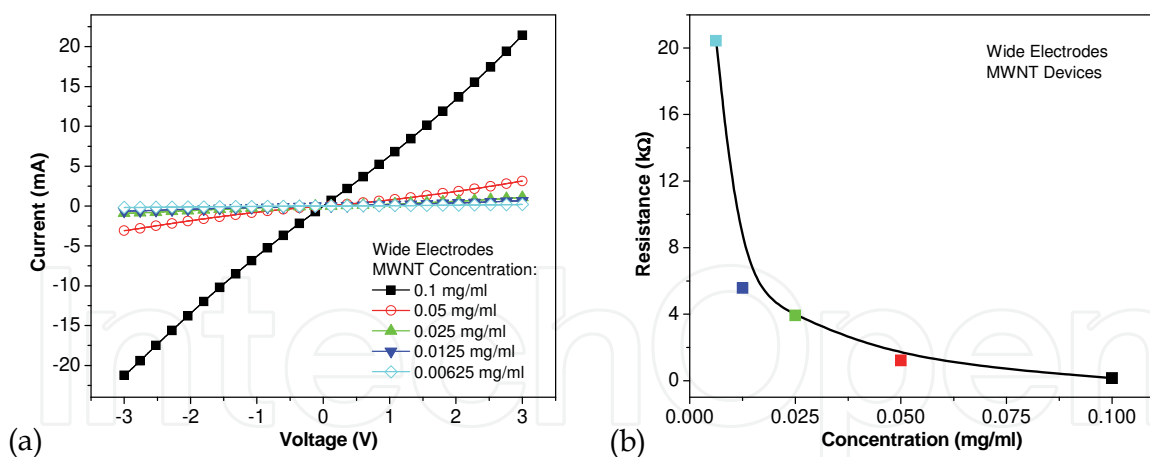


Fig. 16. (a) Current-voltage plots of five devices with the 400- $\mu\text{m}$ -wide electrodes using MWNT solutions with different concentrations. (b) Resistance as a function of the concentration for the aligned MWNTs. The resistances are calculated from (a). Reprinted with permission from P. Li & Xue, 2010b. © 2010 American Society of Mechanical Engineers.

Figure 16 shows the  $I$ - $V$  plots and the resistance-concentration function of the five MWNT devices with the wide electrodes. The MWNT thin films behave in a similar way to the SWNT thin films. At a low MWNT concentration of 0.00625 mg/ml, the resistance is measured as 20.433 k $\Omega$ . As the solution concentration increases, the resistance decreases to

5.576 k $\Omega$  (MWNT solution: 0.0125 mg/ml), 3.926 k $\Omega$  (MWNT solution: 0.025 mg/ml), 1.220 k $\Omega$  (MWNT solution: 0.05 mg/ml), and 0.154 k $\Omega$  (MWNT solution: 0.1 mg/ml).

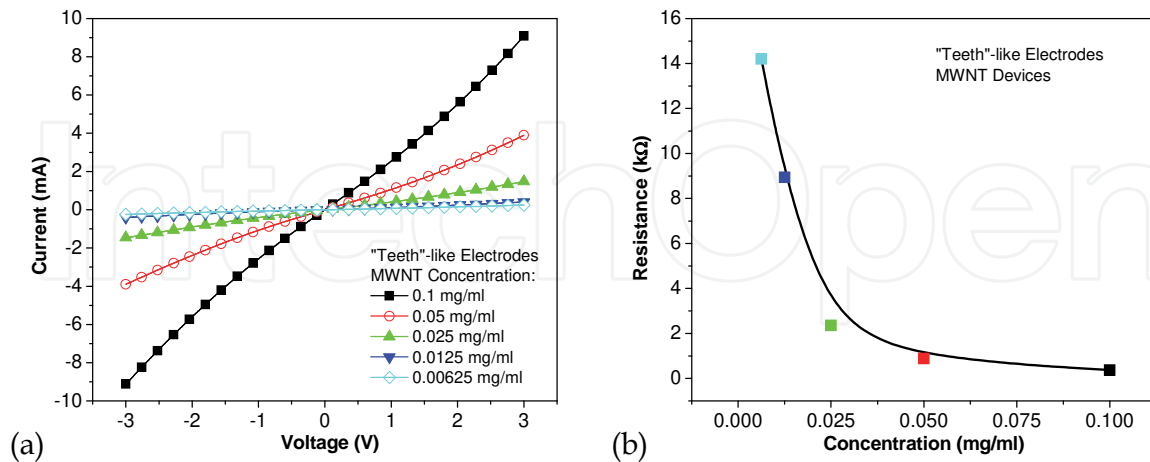


Fig. 17. (a) Current-voltage plots of five devices with the “teeth”-like electrodes using MWNT solutions with different concentrations. (b) Resistance as a function of the concentration for the aligned MWNTs. The resistances are calculated from (a).

The devices with the “teeth”-like electrodes demonstrate similar results, as shown in Fig. 17. The resistance of the devices decreases from 14.201 k $\Omega$  (MWNT solution: 0.00625 mg/ml) to 8.938 k $\Omega$  (MWNT solution: 0.0125 mg/ml), 2.356 k $\Omega$  (MWNT solution: 0.025 mg/ml), 0.890 k $\Omega$  (MWNT solution: 0.05 mg/ml), and 0.374 k $\Omega$  (MWNT solution: 0.1 mg/ml).

However, the  $I$ - $V$  plots of the MWNT devices are not as linear as those of the SWNT devices. The plots show slight curvature in the measurement range of -3 to 3 V. One possible reason for the nonlinearity is that the MWNTs tend to tangle with each other. Therefore, many semiconducting MWNTs are mixed in the bundles and deposited on the substrates during the dielectrophoresis process.

The calculated resistances of the CNTs deposited under different conditions are listed in Table 1. The values are obtained from the electrical characterization of various samples. This table summarizes the results from two materials: SWNTs and MWNTs, two electrode designs: wide electrodes and “teeth”-like electrodes, and six solution concentrations. It can also be used as a reference for future electronics design and experiments.

Our experiments show that the selective deposition of CNTs, including both SWNTs and MWNTs, are highly repeatable. The alignment of CNT thin films, bundles, and individual nanotubes can be achieved using different combinations of solution concentrations and electrode designs. The method presented here can be used in the fabrication of novel CNT-based nanoelectronic devices. Furthermore, we believe that it can also be used in the development of devices beyond electronics, providing a wide range of opportunities. For example, the devices with a controlled amount of CNTs can be used as high-performance sensors for chemical sensing, gas detection, and DNA analysis.

Even though the fabrication and deposition steps presented in this article are still used for small-scale processes, they can be easily extended to large-scale device production. In addition, because the entire process is compatible with the traditional microfabrication technology, it has a high potential to be used in wafer-level fabrication to produce identical devices across the entire surface of the substrate.

Concentration (mg/ml)	Resistance (k $\Omega$ )			
	SWNTs		MWNTs	
	Wide electrodes	"Teeth"-like electrodes	Wide electrodes	"Teeth"-like electrodes
0.2	0.035	0.097	n/a	n/a
0.1	0.099	0.571	0.154	0.374
0.05	0.832	1.256	1.220	0.890
0.025	23.641	2.806	3.926	2.356
0.0125	32.015	11.055	5.576	8.938
0.00625	n/a	n/a	20.433	14.201

Table 1. The calculated resistances of the deposited SWNTs and MWNTs from the electrical characterization.

### 4.3 CNT deposition without an electric field

In order to verify the dielectrophoretic effects on the CNT deposition and alignment, two experiments are conducted for control purposes. Unfortunately, the natural deposition of the CNTs on the substrate is a slow process, resulting in sparsely distributed CNTs across the entire surface. It is difficult to locate the deposited CNTs with the SEM. Therefore, an alternative approach needs to be used.

Because the functionalized CNTs are negatively charged with the covalently attached carboxylic groups, the deposition of CNTs can be enhanced by using substrates with pre-charged surfaces. In this study, we use poly (dimethyldiallylammonium chloride) (PDDA), a positively charged polyelectrolyte, to pre-charge the surface of the silicon substrate (Xue & Cui, 2007). First, the substrate with the 400- $\mu\text{m}$ -wide electrodes is submerged in the PDDA solution for 10 minutes. Next, a drop of CNT solution (with a concentration of 0.1 mg/ml) is placed over the electrodes for 15 min to allow the CNTs to fully deposit on the substrate. Afterward, the substrate is rinsed with DI water and dried with compressed air. Figure 18 shows the SEM images of random networks for both the SWNTs and the MWNTs. In this case, the CNTs cover the entire substrate surface including the gap and the electrodes. There is no CNT alignment observed from these SEM images. Therefore, we can conclude that the alignment of the CNTs in our investigation is solely caused by the dielectrophoresis process.

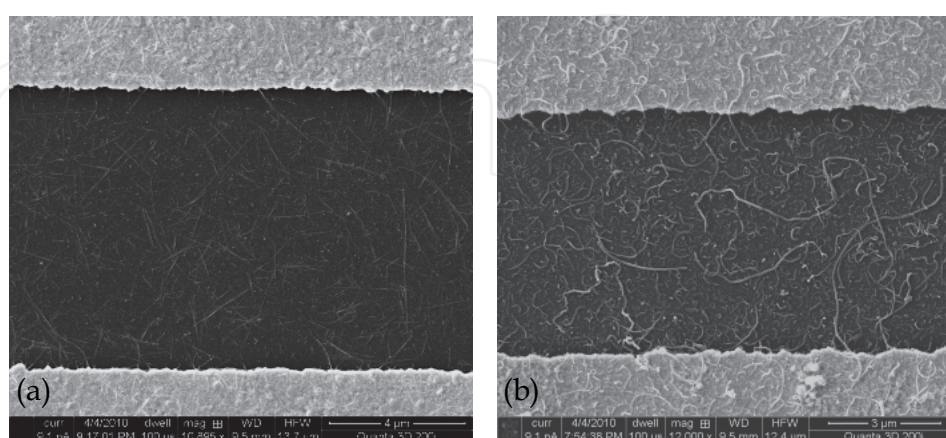


Fig. 18. SEM images (a) a SWNT random network and (b) a MWNT random network. Reprinted with permission from P. Li & Xue, 2010b. © 2010 American Society of Mechanical Engineers.

## 5. Conclusion

In conclusion, we have investigated the dielectrophoretic deposition of SWNTs and MWNTs to obtain organized nanotubes. The deposited and aligned CNTs exist in three forms: thin films, small bundles, and individual nanotubes. The different alignment results are obtained by using various electrode designs and CNT solutions with various concentrations. In general, electrodes with large widths generate an evenly distributed electric field with parallel field lines; the aligned CNTs are in the form of thin films or sparsely distributed bundles. For electrodes with small width, the electric field is highly concentrated and can induce individual nanotube deposition and alignment. The electrical characterization of the aligned SWNTs shows high linearity between the current and voltage; this means that most deposited SWNTs are metallic. However, the current-voltage curves of the MWNTs are curved; this suggests that more semiconducting MWNTs are mixed in the deposited nanotubes. The measurement data illustrate that the resistance of the aligned CNTs can be adjusted in a wide range. The method presented in this article is inexpensive, reliable, and repeatable. In addition, the fabrication process of the devices is compatible with traditional microfabrication technology; it has a high potential to be used in wafer-level fabrication for the mass production of devices in the future. We believe that our investigation of CNTs can facilitate research activities in this field and enable the development of a wide variety of CNT-based devices such as electronics, sensors, and energy storage and conversion systems.

## 6. Acknowledgment

This work was supported by the Washington State University New Faculty Seed Grant.

## 7. References

- Ahmed, W.; Kooij, E. S.; van Silfhout, A. & Poelsema, B. (2009). Quantitative Analysis of Gold Nanorod Alignment after Electric Field-Assisted Deposition. *Nano letters*, Vol. 9, No. 11, (November 2009), pp. 3786-3794, ISSN 1530-6984
- Banerjee, S.; Hemraj-Benny, T. & Wong, S. S. (2005). Covalent Surface Chemistry of Single-Walled Carbon Nanotubes. *Advanced Materials*, Vol. 17, No. 1, (January 2005), pp. 17-29, ISSN 0935-9648
- Boul, P. J.; Turner, K.; Li, J.; Pulikkathara, M. X.; Dwivedi, R. C.; Sosa, E. D.; Lu, Y.; Kuznetsov, O. V.; Moloney, P.; Wilkins, R.; O'Rourke, M. J.; Khabashesku, V. N.; Arepalli, S. & Yowell, L. (2009). Single Wall Carbon Nanotube Response to Proton Radiation. *The Journal of Physical Chemistry C*, Vol. 113, No. 32, (August 2009), pp. 14467-14473, ISSN 1932-7447
- Di Bartolomeo, A.; Rinzan, M.; Boyd, A. K.; Yang, Y.; Guadagno, L.; Giubileo, F. & Barbara, P. (2010). Electrical Properties and Memory Effects of Field-Effect Transistors from Networks of Single- and Double-Walled Carbon Nanotubes. *Nanotechnology*, Vol. 21, No. 11, (March 2010), pp. 115204, ISSN 0957-4484
- Dimaki, M. & Bøggild, P. (2004). Dielectrophoresis of Carbon Nanotubes Using Microelectrodes: A Numerical Study. *Nanotechnology*, Vol. 15, No. 8, (August 2004), pp. 1095-1102, ISSN 0957-4484
- Gultepe, E.; Nagesha, D.; Casse, B. D. F.; Selvarasah, S.; Busnaina, A. & Sridhar, S. (2008). Large Scale 3D Vertical Assembly of Single-Wall Carbon Nanotubes at Ambient

- Temperatures. *Nanotechnology*, Vol. 19, No. 45, (November 2008), pp. 455309, ISSN 0957-4484
- Hu, L.; Choi, J. W.; Yang, Y.; Jeong, S.; La Mantia, F.; Cui, L.-F. & Cui, Y. (2009). Highly Conductive Paper for Energy-Storage Devices. *Proceedings of the National Academy of Sciences of the United States of America*, Vol. 106, No. 51, (December 2009), pp. 21490-21494, ISSN 1091-6490
- Iijima, S. (1991). Helical Microtubules of Graphitic Carbon. *Nature*, Vol. 354, (November 1991), pp. 56-58, ISSN 0028-0836
- Kaempgen, M.; Chan, C. K.; Ma, J.; Cui, Y. & Gruner, G. (2009). Printable Thin Film Supercapacitors Using Single-Walled Carbon Nanotubes. *Nano letters*, Vol. 9, No. 5, (May 2009), pp. 1872-1876, ISSN 1530-6984
- Katz, E. & Willner, I. (2004). Biomolecule-Functionalized Carbon Nanotubes: Applications in Nanobioelectronics. *ChemPhysChem*, Vol. 5, No. 8, (August 2004), pp. 1084-1104, ISSN 1439-4235
- LeMieux, M. C.; Roberts, M.; Barman, S.; Jin, Y. W.; Kim, J. M. & Bao, Z. (2008). Self-Sorted, Aligned Nanotube Networks for Thin-Film Transistors. *Science*, Vol. 321, No. 5885, (July 2008), pp. 101-104, ISSN 0036-8075
- Li, P. & Xue, W. (2010a). Selective Deposition and Alignment of Single-Walled Carbon Nanotubes Assisted by Dielectrophoresis: From Thin Films to Individual Nanotubes. *Nanoscale Research Letters*, Vol. 5, No. 6, (June 2010), pp. 1072-1078, ISSN 1556-276X
- Li, P. & Xue, W. (2010b). Dielectrophoretic Assembly of Organized Carbon Nanotubes and Thin Films. *Proceedings of the ASME 2010 International Mechanical Engineering Congress & Exposition*, ISBN 978-0-791-83891-4, Vancouver, British Columbia, Canada, November 12-18, 2010
- Li, S.; Liu, N.; Chan-Park, M. B.; Yan, Y. & Zhang, Q. (2007). Aligned Single-Walled Carbon Nanotube Patterns with Nanoscale Width, Micron-Scale Length and Controllable Pitch. *Nanotechnology*, Vol. 18, No. 45, (November 2007), pp. 455302, ISSN 0957-4484
- Lim, J.-H.; Phiboolsirichit, N.; Mubeen, S.; Deshusses, M. A.; Mulchandani, A. & Myung, N. V. (2010). Electrical and Gas Sensing Properties of Polyaniline Functionalized Single-Walled Carbon Nanotubes. *Nanotechnology*, Vol. 21, No. 7, (February 2010), pp. 75502, ISSN 0957-4484
- Liu, H.; Takagi, D.; Chiashi, S. & Homma, Y. (2009). The Controlled Growth of Horizontally Aligned Single-Walled Carbon Nanotube Arrays by a Gas Flow Process. *Nanotechnology*, Vol. 20, No. 34, (August 2009), pp. 345604, ISSN 0957-4484
- Monica, A. H.; Papadakis, S. J.; Osiander, R. & Paranjape, M. (2008). Wafer-Level Assembly of Carbon Nanotube Networks Using Dielectrophoresis. *Nanotechnology*, Vol. 19, No. 8, (February 2008), pp. 085303, ISSN 0957-4484
- Mureau, N.; Mendoza, E.; Silva, S. R. P.; Hoettges, K. F. & Hughes, M. P. (2006). *In Situ* and Real Time Determination of Metallic and Semiconducting Single-Walled Carbon Nanotubes in Suspension via Dielectrophoresis. *Applied Physics Letters*, Vol. 88, No. 24, (June 2006), pp. 243109, ISSN 0003-6951
- Padmaraj, D.; Zagozdzon-Wosik, W.; Xie, L.-M.; Hadjiev, V. G.; Cherukuri, P. & Wosik, J. (2009). Parallel and Orthogonal E-field Alignment of Single-Walled Carbon Nanotubes by AC Dielectrophoresis. *Nanotechnology*, Vol. 20, No. 3, (January 2009), pp. 035201, ISSN 0957-4484

- Peng, N.; Zhang, Q.; Li, J. & Liu, N. (2006). Influences of AC Electric Field on the Spatial Distribution of Carbon Nanotubes Formed between Electrodes. *Journal of Applied Physics*, Vol. 100, No. 2, (July 2006), pp. 024309, ISSN 0021-8979
- Raychaudhuri, S.; Dayeh, S. A.; Wang, D. & Yu, E. T. (2009). Precise Semiconductor Nanowire Placement through Dielectrophoresis. *Nano letters*, Vol. 9, No. 6, (June 2009), pp. 2260-2266, ISSN 1530-6984
- Roberts, M. E.; LeMieux, M. C.; Sokolov, A. N. & Bao, Z. (2009). Self-Sorted Nanotube Networks on Polymer Dielectrics for Low-Voltage Thin-Film Transistors. *Nano letters*, Vol. 9, No. 7, (July 2009), pp. 2526-2531, ISSN 1530-6984
- Robertson, J.; Zhong, G.; Telg, H.; Thomsen, C.; Warner, J. H.; Briggs, G. A. D.; Dettlaff-Weglikowska, U. & Roth, S. (2008). Growth and Characterization of High-Density Mats of Single-Walled Carbon Nanotubes for Interconnects. *Applied Physics Letters*, Vol. 93, No. 16, (October 2008), pp. 163111, ISSN 0003-6951
- Seo, H.; Han, C.; Choi, D.; Kim, K. & Lee, Y. (2005). Controlled Assembly of Single SWNTs Bundle Using Dielectrophoresis. *Microelectronic Engineering*, Vol. 81, No. 1, (July 2005), pp. 83-89, ISSN 0167-9317
- Shim, J. S.; Yun, Y.-H.; Rust, M. J.; Do, J.; Shanov, V., Schulz, M. J. & Ahn, C. H. (2009). The Precise Self-Assembly of Individual Carbon Nanotubes Using Magnetic Capturing and Fluidic Alignment. *Nanotechnology*, Vol. 20, No. 32, (August 2009), pp. 325607, ISSN 0957-4484
- Stokes, P. & Khondaker, S. I. (2008). Local-Gated Single-Walled Carbon Nanotube Field Effect Transistors Assembled by AC Dielectrophoresis. *Nanotechnology*, Vol. 19, No. 17, (April 2008), pp. 175202, ISSN 0957-4484
- Tsukruk, V.; Ko, H. & Peleshanko, S. (2004). Nanotube Surface Arrays: Weaving, Bending, and Assembling on Patterned Silicon. *Physical Review Letters*, Vol. 92, No. 6, (February 2004), pp. 1-4, ISSN 0031-9007
- Wang, Y.; Zhou, Z.; Yang, Z.; Chen, X.; Xu, D. & Zhang, Y. (2009). Gas Sensors based on Deposited Single-Walled Carbon Nanotube Networks for DMMP Detection. *Nanotechnology*, Vol. 20, No. 34, (August 2009), pp. 345502, ISSN 0957-4484
- Xiao, Z. & Camino, F. E. (2009). The Fabrication of Carbon Nanotube Field-Effect Transistors with Semiconductors as the Source and Drain Contact Materials. *Nanotechnology*, Vol. 20, No. 13, (April 2009), pp. 135205, ISSN 0957-4484
- Xue, W. & Cui, T. (2007). Characterization of Layer-by-Layer Self-Assembled Carbon Nanotube Multilayer Thin Films. *Nanotechnology*, Vol. 18, No. 14, (April 2007), pp. 145709, ISSN 0957-4484
- Xue, W. & Cui, T. (2008a). Electrical and Electromechanical Characteristics of Self-Assembled Carbon Nanotube Thin Films on Flexible Substrates. *Sensors And Actuators A: Physical*, Vol. 146, (August 2008), pp. 330-335, ISSN 0924-4247
- Xue, W. & Cui, T. (2008b). A Thin-Film Transistor based Acetylcholine Sensor Using Self-Assembled Carbon Nanotubes and SiO<sub>2</sub> Nanoparticles. *Sensors and Actuators B: Chemical*, Vol. 134, No. 2, (September 2008), pp. 981-987, ISSN 0925-4005
- Xue, W. & Cui, T. (2009). Thin-Film Transistors with Controllable Mobilities based on Layer-by-Layer Self-Assembled Carbon Nanotube Composites. *Solid-State Electronics*, Vol. 53, No. 9, (September 2009), pp. 1050-1055, ISSN 0038-1101

- Xue, W.; Liu, Y. & Cui, T. (2006). High-Mobility Transistors based on Nanoassembled Carbon Nanotube Semiconducting Layer and SiO<sub>2</sub> Nanoparticle Dielectric Layer. *Applied Physics Letters*, Vol. 89, No. 16, (October 2006), pp. 1635-1638, ISSN 0003-6951
- Yuen, F. L.-Y.; Zak, G.; Waldman, S. D. & Docoslis, A. (2008). Morphology of Fibroblasts Grown on Substrates formed by Dielectrophoretically Aligned Carbon Nanotubes. *Cytotechnology*, Vol. 56, No. 1, (January 2008), pp. 9-17, ISSN 0920-9069
- Zhou, R.; Wang, P. & Chang, H.-C. (2006). Bacteria Capture, Concentration and Detection by Alternating Current Dielectrophoresis and Self-Assembly of Dispersed Single-Wall Carbon Nanotubes. *Electrophoresis*, Vol. 27, No. 7, (April 2006), pp. 1376-1385, ISSN 0173-0835

IntechOpen



## **Carbon Nanotubes - Synthesis, Characterization, Applications**

Edited by Dr. Siva Yellampalli

ISBN 978-953-307-497-9

Hard cover, 514 pages

**Publisher** InTech

**Published online** 20, July, 2011

**Published in print edition** July, 2011

Carbon nanotubes are one of the most intriguing new materials with extraordinary properties being discovered in the last decade. The unique structure of carbon nanotubes provides nanotubes with extraordinary mechanical and electrical properties. The outstanding properties that these materials possess have opened new interesting researches areas in nanoscience and nanotechnology. Although nanotubes are very promising in a wide variety of fields, application of individual nanotubes for large scale production has been limited. The main roadblocks, which hinder its use, are limited understanding of its synthesis and electrical properties which lead to difficulty in structure control, existence of impurities, and poor processability. This book makes an attempt to provide indepth study and analysis of various synthesis methods, processing techniques and characterization of carbon nanotubes that will lead to the increased applications of carbon nanotubes.

### **How to reference**

In order to correctly reference this scholarly work, feel free to copy and paste the following:

Wei Xue and Pengfei Li (2011). Dielectrophoretic Deposition and Alignment of Carbon Nanotubes, Carbon Nanotubes - Synthesis, Characterization, Applications, Dr. Siva Yellampalli (Ed.), ISBN: 978-953-307-497-9, InTech, Available from: <http://www.intechopen.com/books/carbon-nanotubes-synthesis-characterization-applications/dielectrophoretic-deposition-and-alignment-of-carbon-nanotubes>

**INTECH**  
open science | open minds

### **InTech Europe**

University Campus STeP Ri  
Slavka Krautzeka 83/A  
51000 Rijeka, Croatia  
Phone: +385 (51) 770 447  
Fax: +385 (51) 686 166  
[www.intechopen.com](http://www.intechopen.com)

### **InTech China**

Unit 405, Office Block, Hotel Equatorial Shanghai  
No.65, Yan An Road (West), Shanghai, 200040, China  
中国上海市延安西路65号上海国际贵都大饭店办公楼405单元  
Phone: +86-21-62489820  
Fax: +86-21-62489821

© 2011 The Author(s). Licensee IntechOpen. This chapter is distributed under the terms of the [Creative Commons Attribution-NonCommercial-ShareAlike-3.0 License](#), which permits use, distribution and reproduction for non-commercial purposes, provided the original is properly cited and derivative works building on this content are distributed under the same license.

IntechOpen

IntechOpen